



## Combined drug repurposing and virtual screening strategies with molecular dynamics simulation identified potent inhibitors for SARS-CoV-2 main protease (3CLpro)

Abbas Khan<sup>a</sup>, Syed Shujait Ali<sup>b</sup>, Muhammad Tahir Khan<sup>a</sup> , Shoaib Saleem<sup>c</sup>, Arif Ali<sup>a</sup>, Muhammad Suleman<sup>b</sup>, Zainib Babar<sup>d</sup>, Athar Shafiq<sup>a</sup>, Mazhar Khan<sup>e</sup>  and Dong-Qing Wei<sup>a,f,g</sup>

<sup>a</sup>State Key Lab of Microbial Metabolism, Department of Bioinformatics and Biological Statistics, School of Life Sciences and Biotechnology, Shanghai Jiao Tong University, Shanghai, China; <sup>b</sup>Center for Biotechnology and Microbiology, University of Swat, Swat, Pakistan; <sup>c</sup>National Center for Bioinformatics, Quaid-i-Azam University, Islamabad, Pakistan; <sup>d</sup>Center for Viticulture and Enology, School of Agriculture and Biology, Shanghai Jiao Tong University, Shanghai, China; <sup>e</sup>The CAS Key Laboratory of Innate Immunity and Chronic Diseases, Hefei National Laboratory for Physical Sciences at Microscale, School of Life Sciences, CAS Center for Excellence in Molecular Cell Science, University of Science and Technology of China (USTC), Collaborative Innovation Center of Genetics and Development, Hefei, China; <sup>f</sup>State Key Laboratory of Microbial Metabolism, Shanghai-Islamabad-Belgrade Joint Innovation Center on Antibacterial Resistances, Joint Laboratory of International Cooperation in Metabolic and Developmental Sciences, Ministry of Education and School of Life Sciences and Biotechnology, Shanghai Jiao Tong University, Shanghai, P.R. China; <sup>g</sup>Peng Cheng Laboratory, Shenzhen, P.R. China

Communicated by Ramaswamy H. Sarma.

### ABSTRACT

The current coronavirus (SARS-CoV-2) pandemic and phenomenal spread to every nook and cranny of the world has raised major apprehensions about the modern public health care system. So far as a result of this epidemic, 4,434,653 confirmed cases and 302,169 deaths are reported. The growing infection rate and death toll demand the use of all possible approaches to design novel drugs and vaccines to curb this disease. In this study, we combined drugs repurposing and virtual drug screening strategies to target 3CLpro, which has an essential role in viral maturation and replication. A total of 31 FDA approved anti-HIV drugs, and Traditional Chinese medicines (TCM) database were screened to find potential inhibitors. As a result, Saquinavir, and five drugs (TCM5280805, TCM5280445, TCM5280343, TCM5280863, and TCM5458190) from the TCM database were found as promising hits. Furthermore, results from molecular dynamics simulation and total binding free energy revealed that Saquinavir and TCM5280805 target the catalytic dyad (His41 and Cys145) and possess stable dynamics behavior. Thus, we suggest that these compounds should be tested experimentally against the SARS-CoV-2 as Saquinavir has been reported to inhibit HIV protease experimentally. Considering the intensity of coronavirus dissemination, the present research is in line with the idea of discovering the latest inhibitors against the coronavirus essential pathways to accelerate the drug development cycle.

### ARTICLE HISTORY

Received 14 April 2020  
Accepted 3 June 2020

### KEYWORDS

SARS-CoV-2; 3CLpro; drug-repurposing; virtual screening; binding free energy

### Introduction

The Coronaviruses (CoVs) are placed within four Genera, Alpha-coronavirus, Beta-coronavirus, Gamma-coronavirus and Delta-coronavirus ( $\alpha$ ,  $\beta$ ,  $\gamma$ , and  $\delta$ ) of subfamily Orthocoronavirinae. However, the members of Beta-coronavirus such as severe acute respiratory syndrome coronavirus (SARS-CoV1 and SARS-CoV2) and the Middle East Respiratory Syndrome Coronavirus (MERS-CoV) have been involved in pneumonia epidemics in the 21st century. SARS-CoV1, MERS-CoV and SARS-CoV2 outbreaks caused by zoonotic viruses (Lau et al., 2005; Reusken et al., 2013); in 2003, 2012 and 2019–20 with the case fatality ratio of 10% (Cheng et al., 2007; Lee et al., 2003; Zaki et al., 2012), 35% (de Groot et al., 2013; Zaki et al., 2012); and 5%, respectively. The recent outbreak and phenomenal spread of SARS-CoV-2 to every nook and cranny of the world (3.66 million infections and 309774 deaths) compelled World Health Organization (WHO) to

declare it pandemic on March 20, 2020. The virus causing covid-19 was named 2019-nCoV (2019 novel coronavirus) on January 12, 2020 by WHO (Chen et al., 2020; Zhu et al., 2020), however the International Virus Classification Commission (ICTV) on February 11, 2020, named this virus as Severe Acute Respiratory Syndrome Coronavirus 2 (SARS-CoV-2). This threat of global concern to humanity, mainly due to the unavailability of proper treatment (Huang et al., 2020) pushed the investigators to discover and design therapeutic drugs and vaccines to combat the coronavirus. Infection symptoms include fever, dyspnea, shortness of breath, and cough, whereas severe cases lead to kidney failure and death (Rothan & Byrareddy, 2020).

The SARS-CoV-2 is composed of Spike (S) protein, membrane (M) protein, envelope (E) protein, and nucleocapsid (N) protein. In anti CoVs therapies, the main focus is to boost the human immune system or to block the binding of spike protein with the receptor proteins. Therefore, the treatments

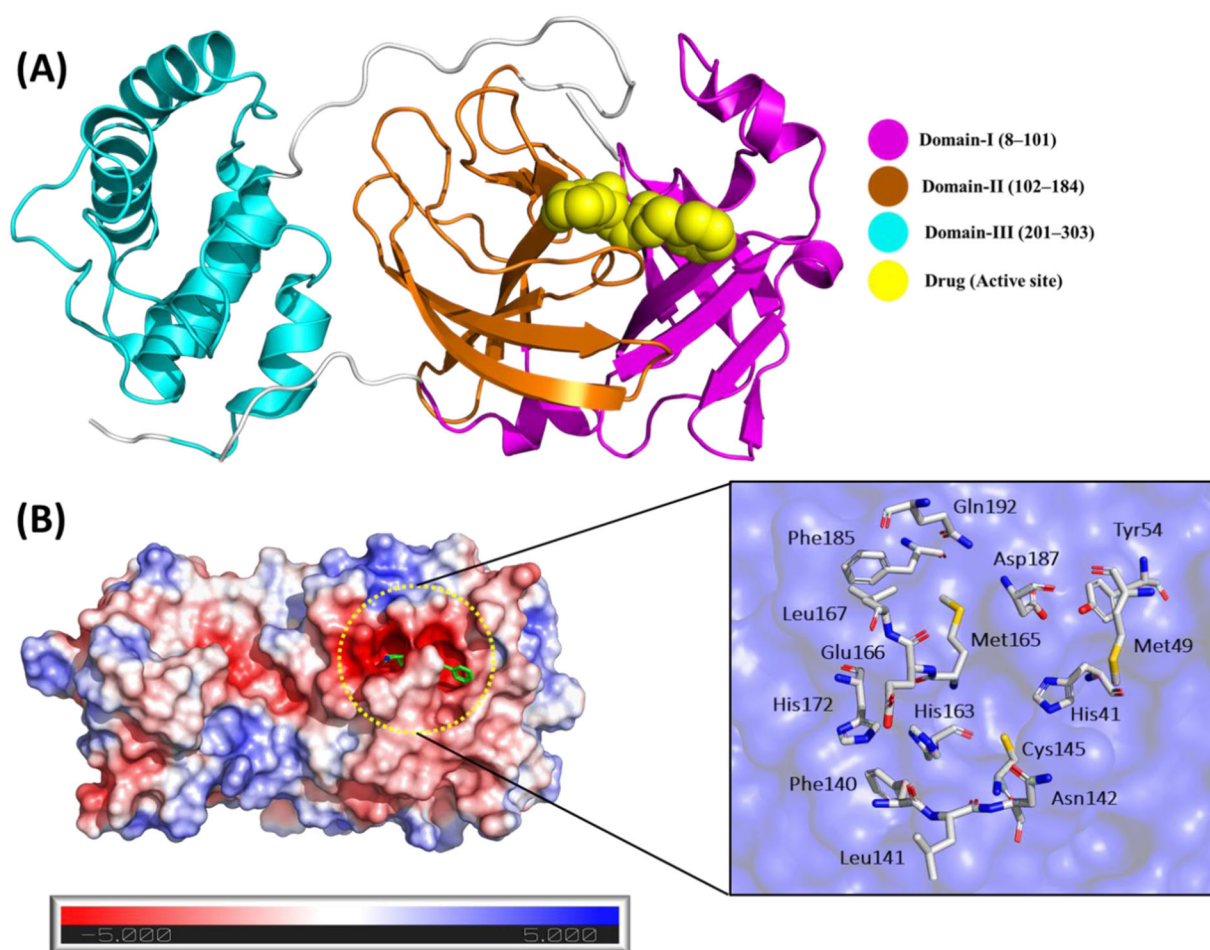


**Figure 1.** Structure of 3CLpro (SARS-COV-2) retrieved from RCSB using accession number (6LU7). (A) showing the domains architecture of three different domains. (Domain 1) magenta, (Domain 2) orange, (Domain 3) cyan, (Connecting loops) grey while the drug molecule in the active site is shown in yellow colour as sphere. (B) The electrostatic potential of 3CLPro and displays the important active site residues in the sticks, including the two essential residues His41 and Cys145 (catalytic dyad).

based on targeting coronavirus rely on blocking of virus binding to receptors, inhibition of virus replication, prevention of the synthesis of viral RNA and inhibition of the virus self-assembly process (Bosch et al., 2003; Khan et al., 2018; Omrani et al., 2014).

To combat the latest CoVs threats, the researchers are following multiple approaches for novel drug development (Zumla et al., 2016) and testing the efficacy of existing drugs. In one approach, experiments were performed to test the existing broad-spectrum antiviral drugs (ribavirin, Interferons, and cyclophilin inhibitors) against SARS-COV-2 (Chan et al., 2013; Zumla et al., 2016). The use of these antiviral drugs is approved against viral infections, and their dosages, efficacy, metabolic characteristic, and side effects are well known. However, there is a possibility that this “broad-spectrum” treatment against CoVs would not be effective. In the second approach, molecular databases were subjected to High-throughput screening for potential drug molecules to combat infection caused by a coronavirus (de Wilde et al., 2014; Dyall et al., 2014). This strategy was proved successful in the discovery of lopinavir/ritonavir for the treatment of HIV. Some researchers are using the genomic and pathological information of CoVs for the development of a new specific drug from scratch. Theoretically, this is an effective approach; however, it

is very time consuming and might cost several years or even more than ten years (Khan et al., 2018; Omrani et al., 2014).

Structural Bioinformatics based approaches are the fastest way for finding the potential molecules from the marketed drugs or bioactive compounds for effective treatment of SARS-COV-2. Main-protease or 3CLpro inhibition is a promising target to control the recent SARS-COV-2 infection due to its essential role in viral maturation and replication (Ul Qamar et al., 2020). 3CLpro has three important domains I-III, which correspond to positions 8–101, 102–184, and 201–303, respectively. There is a connecting loop that corresponds to position 185–200, which connects domains II and III. The structure of 3CLpro has an important catalytic dyad consist of His41 and Cys145. In this study, the protein of SARS-COV-2 (3CLpro, also named 3-chymotrypsin-like protease) was subjected to drug repurposing and virtual screening for potent drug identification followed by molecular dynamics simulation and binding free energy calculation. Our findings revealed that Saquinavir, which is an HIV protease inhibitor reported experimentally (Kim et al., 1998) and TCM5280805, are promising hits, which need *in vitro* validation for antiviral effects. We hope this study will provide useful information for the clinical treatment of novel coronavirus associated pneumonia.

## Materials and methods

### Protein and ligand structure preparation

Protein databank (<http://www.rcsb.org/>) (Rose et al., 2016) was used for retrieval of 3CLpro (6LU7) crystal structure. Using the protein preparation implemented in Schrödinger software (Schrödinger, LLC, New York, NY), the structure was prepared and optimized. The OPLS\_2005 force field was used for protein-energy minimization. For ligands preparation such as assigning appropriate ionization, stereochemistry, ring conformations, and tautomer (Release, 2017; Schrodinger, 2011), a LigPrep module was used. APBS tool (Lerner & Carlson, 2006) implemented in PyMOL was used for electrostatic potential calculation.

### Repurposing of anti-HIV drugs against 3CLpro

Drug repositioning or repurposing approach is used to speed up the drug development cycle by finding a new therapeutic application for a marketed drug that has been licensed for a particular use (Sleigh & Barton, 2010). This approach was fruitful in the case of sildenafil for leprosy, erectile dysfunction, and pulmonary hypertension, and multiple myeloma thalidomide (Hernandez et al., 2017). Literature mining was carried out to collect anti-HIV drugs for screening against 3CLpro (SARS-COV-2). Multiple drugs were retrieved from drugbank database. A total of 31 drugs were shortlisted for screening against the 3CLpro (SARS-COV-2).

### High-throughput virtual screening

Schrödinger binding site was used for finding the binding site of proteins using the default parameters, and the generated maps show the binding cavity. The identified binding sites have the descriptions regarding hydrogen bonding, a degree of exposure and enclosure, size, linking site points, tightness, hydrophobic and hydrophilic nature. The grid with dimensions  $12 \text{ \AA} \times 12 \text{ \AA} \times 12 \text{ \AA}$  was generated. The final active site grid identified was based on the experimentally reported residues by a recent crystallographic study (Jin et al., 2020) and the maps generated by Schrödinger Maestro. Three steps of virtual screening (HTVS, SP, and XP) were used to screen the anti-HIV and TCM compounds databases. Furthermore, the bioactivity of these compounds was predicted by using molinspiration cheminformatics tool. Molinspiration is an efficient tool that has been used by several studies (~4500) to predict bioactivity results.

### Molecular dynamics simulation of protein-ligand complexes

Top hits from anti-HIV drugs and TCM database were subjected to molecular dynamics simulation using the Amber18 package (Case et al., 2005). The antechamber was used to generate the drugs topologies. TIP3P water model was to solvate the system, and Na<sup>+</sup> counter ions were used to neutralizing the system. Two steps energy minimization of the system followed by heating and equilibration was performed.

**Table 1.** A list of anti-HIV drugs used for docking against the proteinase enzyme of coronavirus (SARS-COV-2).

Drug Name	Drugbank ID	Targeted virus(es)			
		HIV-1	HIV-II	HBV	HTLV-1
Enfuvirtide	DB00109	✓	X	X	X
Nelfinavir	DB00220	✓	X	X	X
Indinavir	DB00224	✓	X	X	✓
Nevirapine	DB00238	✓	X	X	X
Tenofoviridisoproxil	DB00300	✓	X	X	X
Zidovudine	DB00495	✓	X	X	X
Ritonavir	DB00503	✓	X	X	X
Efavirenz	DB00625	✓	X	X	X
Stavudine	DB00649	✓	X	X	X
Amprenavir	DB00701	✓	✓	X	X
Delavirdine	DB00705	✓	X	X	X
Lamivudine	DB00709	✓	X	✓	X
Emtricitabine	DB00879	✓	X	X	X
Didanosine	DB00900	✓	X	X	X
Tipranavir	DB00932	✓	X	X	X
Zalcitabine	DB00943	✓	X	X	X
Abacavir	DB01048	✓	X	X	X
Atazanavir	DB01072	✓	X	X	X
Saquinavir	DB01232	✓	X	X	X
Darunavir	DB01264	✓	✓	X	X
Fosamprenavir	DB01319	✓	X	X	X
Lopinavir	DB01601	✓	X	X	X
Inosine pranobex	DB04335	✓	X	X	X
Maraviroc	DB04835	✓	X	X	X
Etravirine	DB06414	✓	X	X	X
Raltegravir	DB06817	✓	X	X	X
Rilpivirine	DB08864	✓	X	X	X
Dolutegravir	DB08930	✓	X	X	X
Cobicistat	DB09065	✓	X	X	X
Elvitegravir	DB09101	✓	X	X	X
Tenofovirafenamide	DB09299	✓	X	✓	X

Particle Mesh Ewald (PME) algorithm was applied to calculate the long-range electrostatic interactions (Price & Brooks III, 2004). For Van der Waals interactions, a 1.4 nm cutoff values were set and also for short-range Columbic, respectively. A total of 100 ns MD simulation was performed with a time step of 2 fs. The behavior of the ligand-protein complex and stability were analyzed. Post-simulation analysis such as RMSD, RMSF, ROG and hydrogen bonds occupancy were performed using CPPTRAJ and PTRAJ (Roe & Cheatham III, 2013).

### The binding free energy calculations

The script MMPBSA.PY was used to calculate the free binding energy for all the protein-ligand complexes (Chen et al., 2016; Hou et al., 2012; Miller III et al., 2012; Sun et al., 2014); considering 500 snapshots from MD trajectories using the following equation:

$$\Delta G_{bind} = \Delta G_{complex} - [\Delta G_{receptor} + \Delta G_{ligand}]$$

In this equation,  $\Delta G_{bind}$  represents total free binding energy, while others show the free energy of complex, the protein, and the ligand. Specific energy term contributes to the whole Free energy was calculated by the equation:

$$G = G_{bond} + G_{ele} + G_{vdW} + G_{pol} + G_{npol} - TS$$

$G_{bond}$ ,  $G_{ele}$  and  $G_{vdW}$  specify interactions among bonded, electrostatic, and van der Waals states. In contrast,  $G_{pol}$  and  $G_{npol}$  represent the polar and non-polar interaction to the

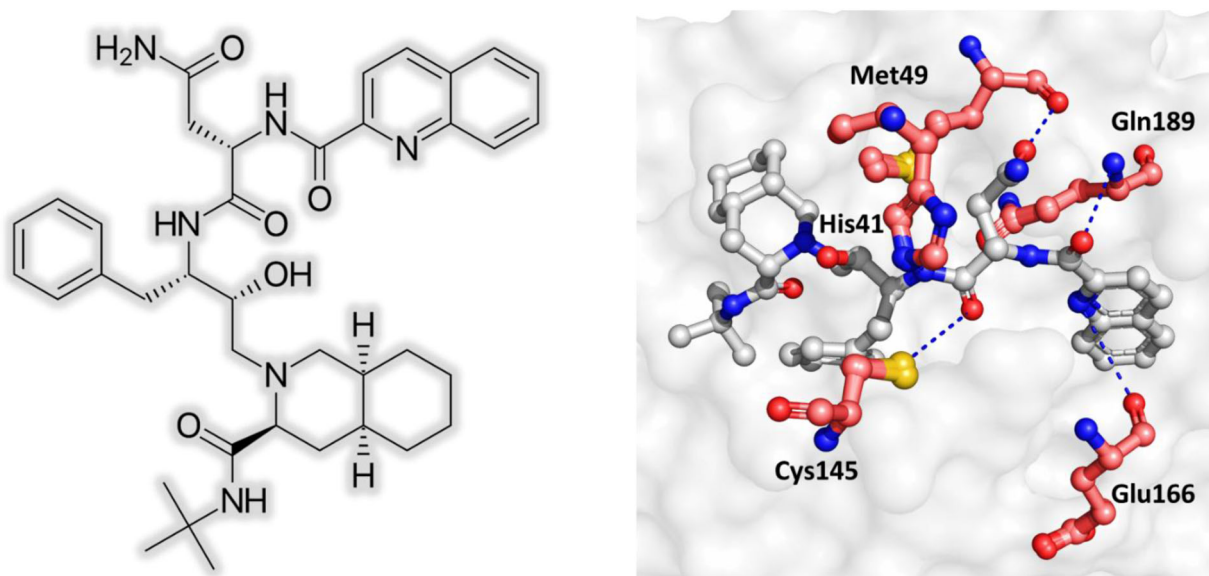


**Figure 2.** Interaction pattern of Saquinavir with the SARS-COV-2 proteinase. The left panes show the Saquinavir drug in 2D, while the right panel shows the interaction of Saquinavir with the critical active site residues, including His41 and Cys145.

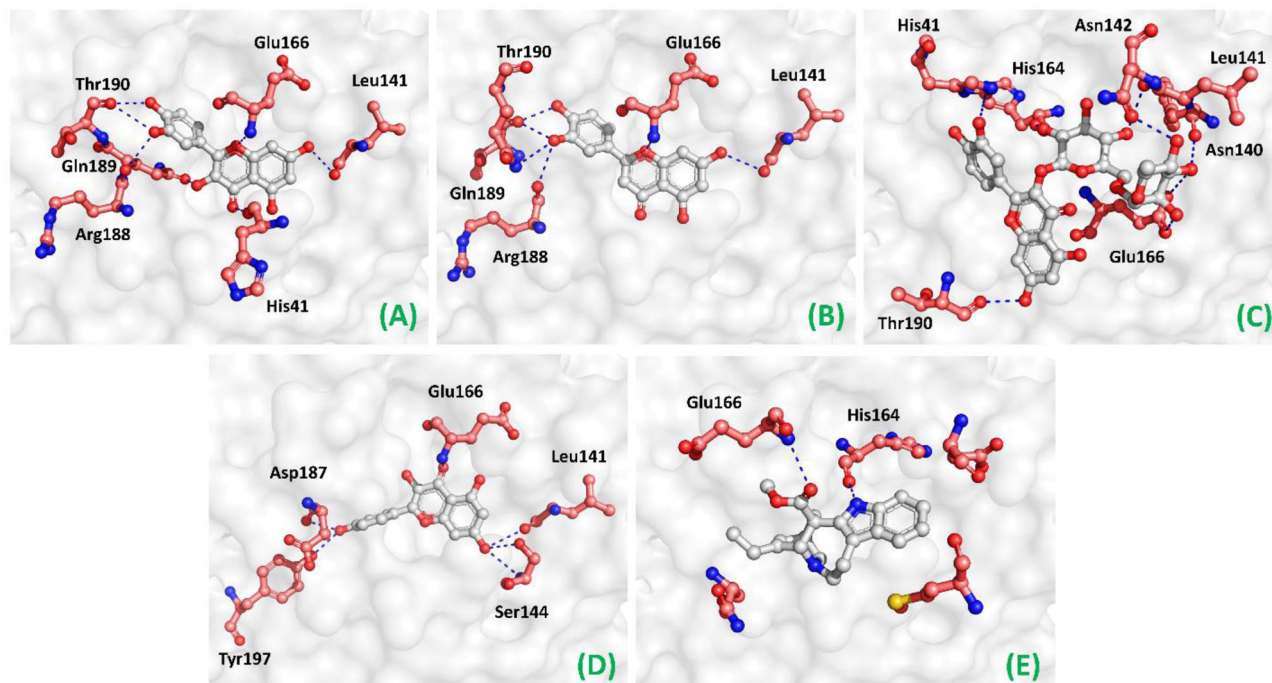


**Figure 3.** Interaction pattern of the top five compounds from the TCM database. (A) 5280343, (B) 5280445, (C) 5280805, (D) 5280863 and (E) 5458190.

free energy presumed through precise GB (Generalized Born). This free energy calculation method is widely used by different studies to understand the binding energy of different ligands (Khan et al., 2019; Wang et al., 2019).

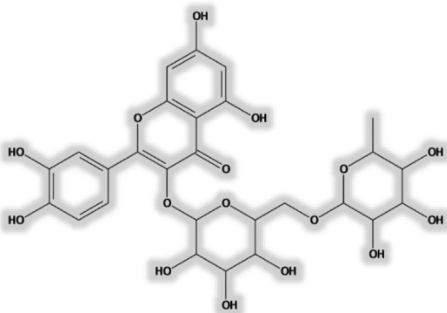
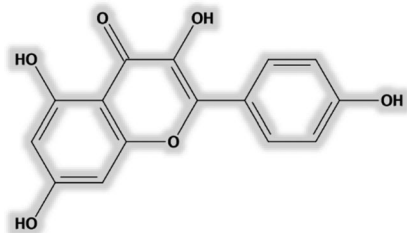
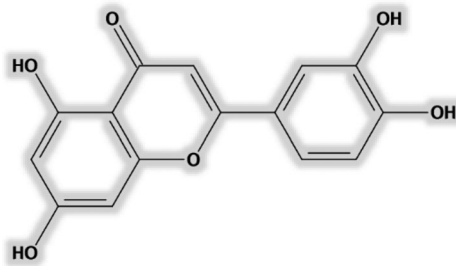
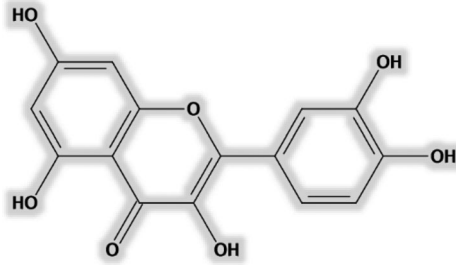
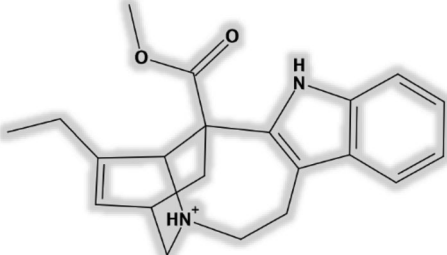
## Results and discussion

### 3CLpro structure retrieval and preparation

The crystallographic structure (306 amino acids long) of the 3CLpro (SARS-COV-2) was retrieved from the RCSB database using accession ID: 6LU7. The structure of 3CLpro was analyzed for missing residues and refinement. The structure was

subjected to energy minimization and structure preparation using Maestro. The structure of 3CLpro has three domains, as given in Figure 1(A). These domains I-III correspond to position 8–101, 102–184, and 201–303, respectively. While there is a connecting loop corresponds to position 185–200, which connects domains II and III. All these domains are coloured differently. The ligand in the active site (Yellow colour (sphere)) has also been shown in Figure 1(A). The electrostatic potential of the 3CLPro shows that the active site region possesses a strong electronegative potential, while weak electronegative potential around the active site can also be observed. However, the weak electropositive and neutral potential is distributed too. The active site grid

**Table 2.** 2D coordinates of the top five compounds from TCM database with their docking and bioactivity scores predicted by molinspiration cheminformatics tool.

S. No	Entry ID	2D structure	Docking score	Bioactivity
1.	5280805		-11.183	-0.07
2.	5280863		-7.688	-0.27
3.	5280445		-7.624	-0.22
4.	5280343		-7.434	-0.25
5.	5458190		-7.126	-0.12

( $X = -10.71$ ,  $Y = 12.41$ ,  $Z = 68.83$ ) was generated, and important residues were identified. Important active site residues His41, Met49, Tyr54, Phe140, Leu141, Asn142, Cys145, His163,

Met165, Glu166, Leu167, Phe185, Asn187, and Gln192 were identified and shown in [Figure 1\(B\)](#). The binding cleft is at the same place as in the previously reported SARS with the

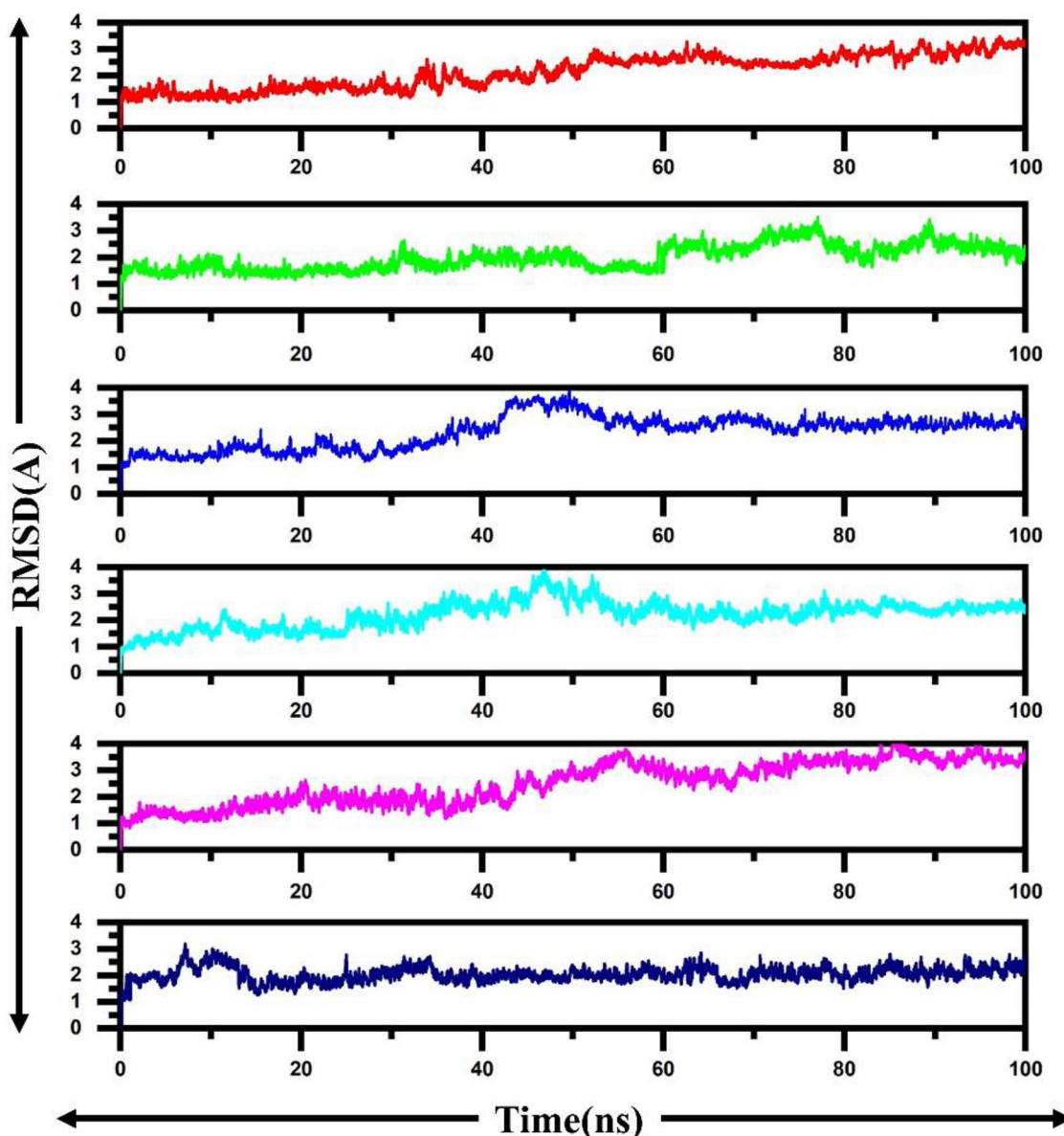


**Figure 4.** RMSDs of all the systems including 3CLpro-Squonavir (red), 3CLpro-5280805 (green), 3CLpro-5280445 (blue), 3CLpro-5280343 (cyan), 3CLpro-5280863 (magenta) and 3CLpro-5458190 (navy). The x-axis shows the time in nanoseconds while the y-axis shows the RMSD in Å.

two critical residues HIS41 and CYS145 forms a catalytic dyad.

### Repurposing anti-HIV drugs against the 3CLpro (SARS-COV-2)

In the current study, the repurposing of anti-HIV drugs against the SARS-COV-2 main protease was carried out using structure-based screening methods. Anti-HIV drugs such as Lopinavir–Ritonavir are reported to be active against the SARS-CoV-2. Clinical trials of these drugs on different groups of patients showed significant improvement. Thus, anti-HIV drugs possess the potential to work against SRS-CoV-2 targets. Therefore, immediate testing of anti-HIV drugs may lead to a discovery of potent inhibitor against the SARS-CoV-2. A list of 31 anti-HIV drugs (Table 1) was downloaded from drugbank database (<https://www.drugbank.ca/>) using their respective accession IDs (Wishart et al., 2018).

These drugs were prepared for molecular docking against the proteinase enzymes of coronavirus (SARS-COV-2). The docking scores were ranged from  $-9.09$  kcal/mol to  $-4.16$  kcal/mol. All the conformations were analyzed for the best interactions with the key residues. Initial criteria were set to shortlist the drugs based on binding affinity and interactions with the dyad residues (His41 and Cys145). The docking score  $-9.09$  kcal/mol was reported for the HIV protease inhibitor drug Saquinavir (Figure 2). This drug has been reported to inhibit the HIV proteinase enzymes too. In this case, (SARS-COV-2), the Saquinavir formed six hydrogen bonds, including two with the central dyad residues (His41 and Cys145). Previous reports on different SARS, such as the octa-peptide, also stressed the blocking of these two residues. Other interactions include four hydrogen bonds with Glu166, Gln189, Met49, and Gly143, while some pi-alkyl interactions, including one with Cys145 and other residues, are also formed. Thus, we speculate that the clinical testing of

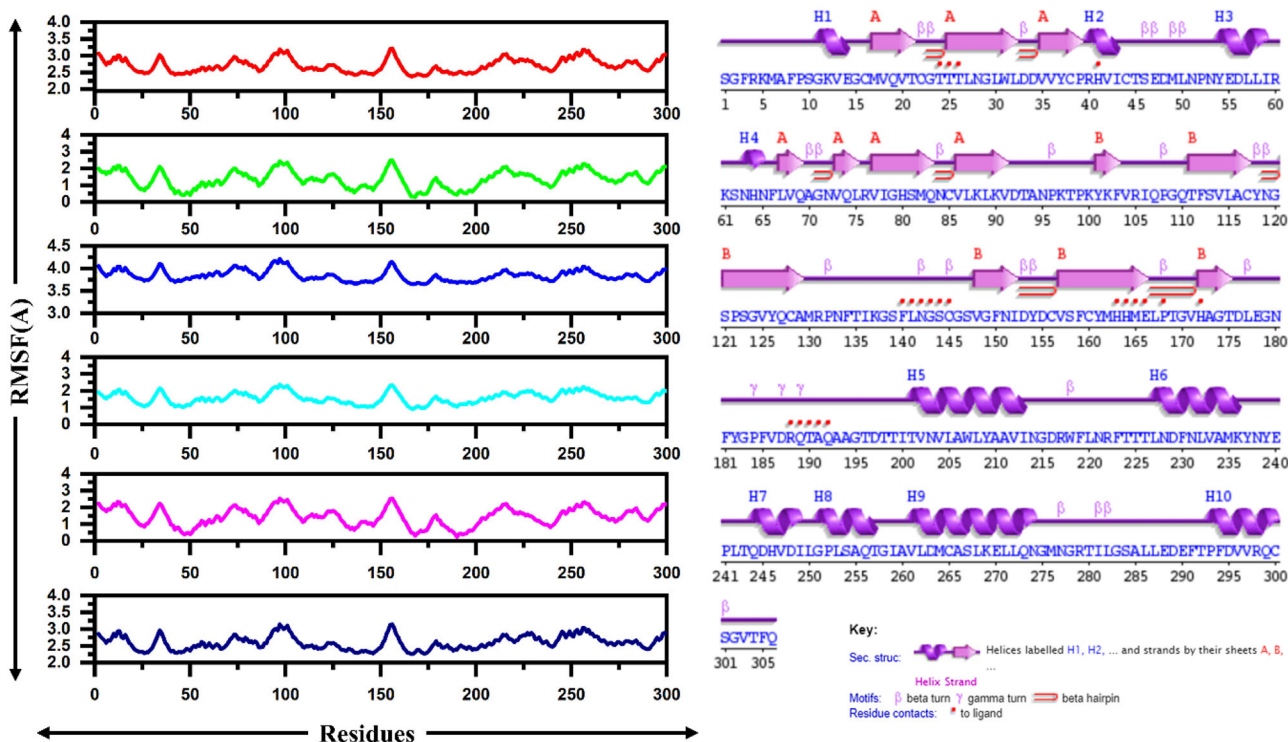


**Figure 5.** RMSFs of all the systems including 3CLpro-Squanavir (red), 3CLpro-5280805 (green), 3CLpro-5280445 (blue), 3CLpro-5280343 (cyan), 3CLpro-5280863 (magenta) and 3CLpro-5458190 (navy). The x-axis shows the time in nanoseconds while the y-axis shows the RMSF in Å. The right panel shows the secondary structure of 3CLpro.

Saquinavir should be done at the earliest. It is also reported by different scientists that HIV drugs could be potentially used against the recent coronavirus.

### Virtual screening of TCM database against the 3CLpro (SARS-COV-2)

Furthermore, we also performed virtual screening of the Traditional Chinese medicines database (TCM). A total of 37,800 compounds were screened after excluding the drugs violating the Lipinski rules of five. Important residues in the active site (His41 and Cys145) were targeted. The top five compounds based on the docking scores were selected. The best docking score,  $-11.183$  kcal/mol, was reported for the compound (5280805). More than ten bonds, including hydrogen bonds, van der Waals, electrostatics, and pi-alkyl interactions, were formed. Among the seven hydrogen bonds, two hydrogen bonds with the residue His41 were also formed, which is a key residue in the active site dyad. Among the other Phe140, Leu141, Asn142, His164, Glu166, and Thr190 also formed hydrogen bonds with the ligand (5280805).

On the other hand, compound 5280863, with the docking score  $-7.688$  kcal/mol formed a strong hydrogen bond with the key residue His41. The compound 5280863 also formed five hydrogen bonds with the other active site residues (Glu166, Arg188, Gln189, and Thr190). The other three compounds (5280445, 5280343, and 5458190) were also analyzed for the interaction with the key residues. It can be seen from Figure 3 that His41 is mainly involved in the interaction with the ligands. Table 2 is showing the 2D structures of the top five compounds with their docking scores.

Cross validation of our predicted compounds by comparing with the experimentally tested compounds showed that the Saquinavir and TCM5280805 possess a similar scaffold with Myricetrin and Scutellarin which are flavonoids and reported to have strong inhibitory effects by targeting 3CLpro. On the other hand, the four compounds (TCM5280343, TCM5280445, TCM5280863 and TCM5458190) from TCM database shares structural similarity with Scutellarein, Dihyromyricetin, Quercetagetin, Myricetin, 5,6-Dihydroxyflavone, 6,7-Dihydroxyflavone, Chrysin, Herbacetin and Baicalein which are flavonoids and testes to have strong inhibitory effects in an experimental condition by targeting 3CLpro (Chen & Du, 2020; Dai et al., 2020; Yang et al., 2020). Their structural analyses showed that these compounds mainly form bonds with Phe140 and Glu166 while our compounds specifically target the catalytic dyad with supplementary interactions with the other active site residues. Thus, we speculate that our compounds could also show the same potential activity against the 3CLpro in the experimental assay because our compounds are also plants derived extracts and belongs to a group of flavonoids.

Furthermore, results obtained from the server shows that all these shortlisted compounds are active against the protease target. From the scores it can be seen that Saquinavir with score 0.40 possesses strong inhibitory effects against the proteases while the others the reported score for TCM5280805 ( $-0.7$ ), TCM5280863 ( $-0.27$ ), TCM5280445 ( $-0.22$ ), TCM5280343 ( $-0.25$ ) while TCM5458190 possess ( $-0.12$ ) bioactivity score against the protease target. Thus, these results strongly suggest that the shortlisted compounds could efficiently inhibit the 3CLPro in the experimental setup and could be tested for clinical trials.

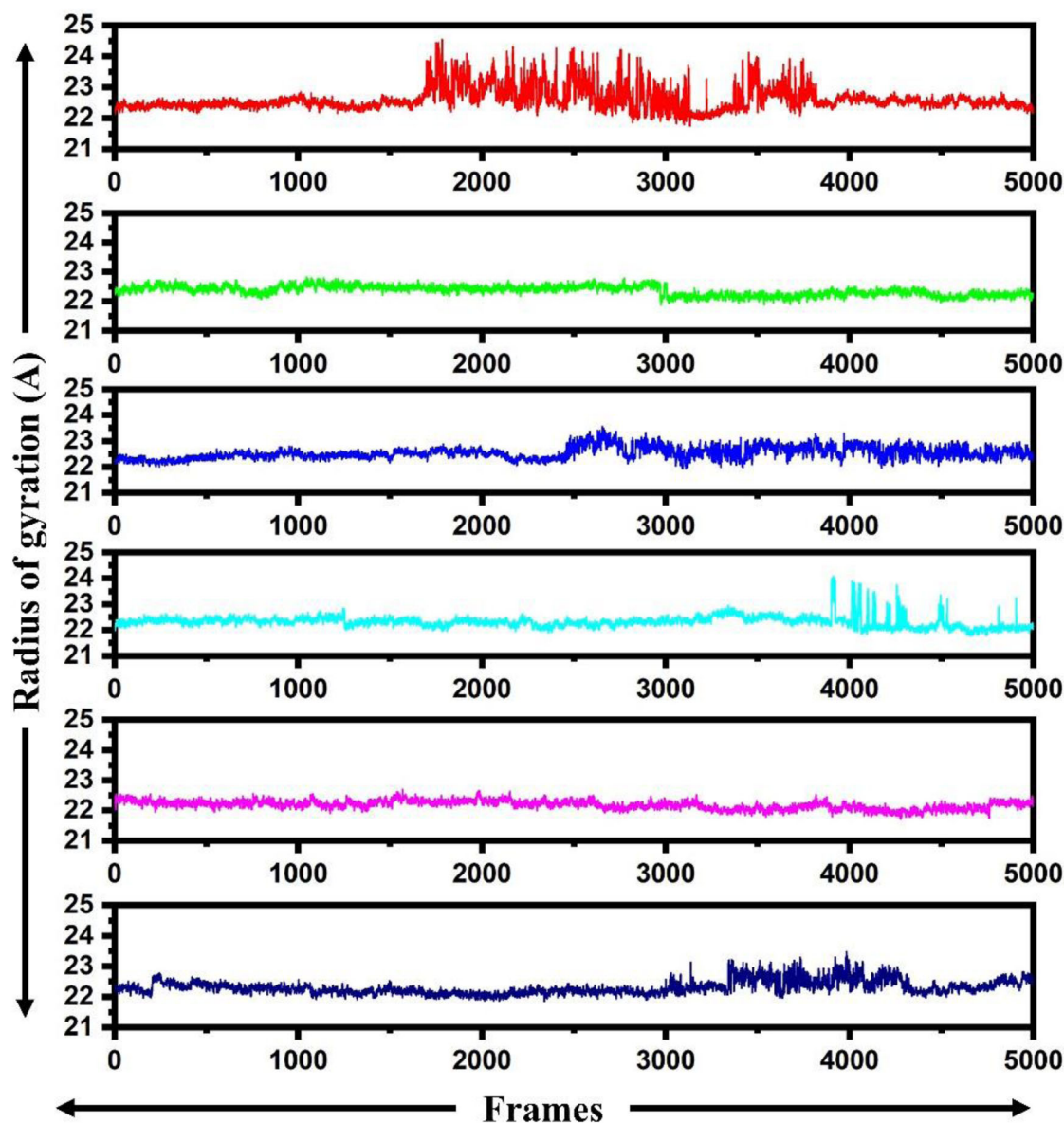


**Figure 6.** RoGs (radius of gyration) of all the systems including 3CLpro-Squanavir (red), 3CLpro-5280805 (green), 3CLpro-5280445 (blue), 3CLpro-5280343 (cyan), 3CLpro-5280863 (magenta) and 3CLpro-5458190 (navy).

### Molecular dynamics simulation of the top hits

To understand the conformational and dynamics features of the selected hits against the 3CLpro of SARS-COV-2 molecular dynamics (MD) simulation is an imperative method to explore the behavior of each system in real-time. Dynamics features of the six selected systems (Saquinavir, 528085, 5280863, 5280445, 5280343, and 5458190) were calculated after 100 ns simulation. For stability RMSD, while to evaluate the flexibility at residue level RMSF of the complexes were calculated to comprehend the overall stability and flexibility of the system.

### RMSD analysis

The stability of all the six systems was calculated by using Root Mean Square Deviation (RMSD). We tested the stability of the docked drugs in the active pocket and its effects on

the stability of the whole system. The results suggest that all the six systems were stable with acceptable deviation (as shown in Figure 4). The average RMSD for all the systems was found to be between 1 and 4 Å. Saquinavir-3CLpro exhibited an average RMSD of 2.5 Å soon after reaching 35 ns; the system attained stability remains uniform for the rest of the time. It can be seen that the complex 3CLpro-5280805 remained stable, but after 60 ns, the system showed an acceptable deviation for a little time. After that, the system gained stability and entered the production stage. For a complex 3CLpro-5280445, the system showed a slight deviation between 40 and 45 ns but remained stable during the course of the simulation.

On the other hand, 3CLpro-5280343 and 3CLpro-5280863 reported divergence between 40 and 60 ns, but the system soon gained stability. Similarly, in the case of 3CLpro-5458190, the examination of RMSD of the C $\alpha$  backbone has an average RMSD of 2.3 Å. The system shows a deviation in



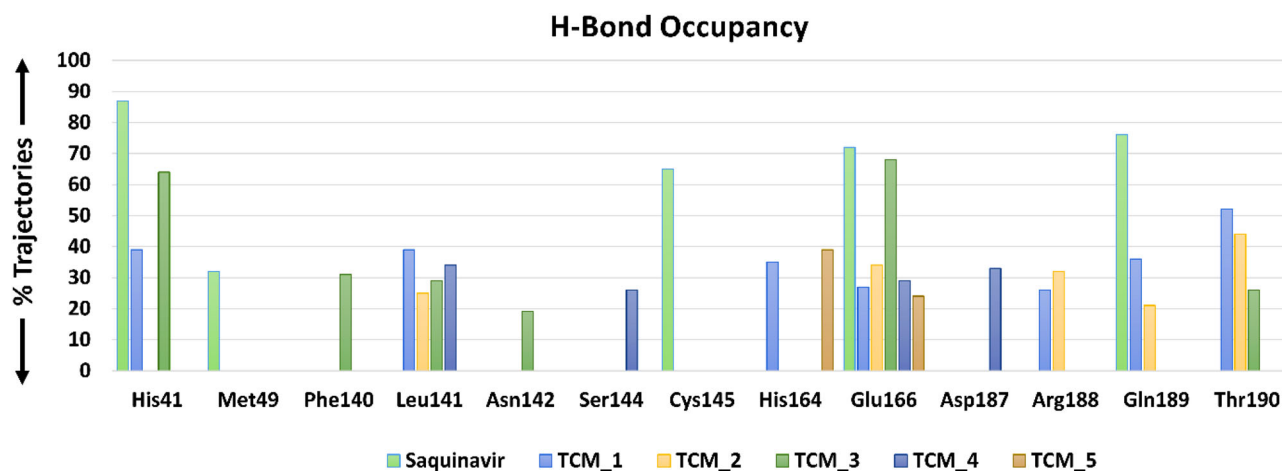


**Figure 7.** Showing the hydrogen bonding occupancy of each complex. His41, Leu141, Glu166, Gln189, and Thr190 were found to be involved in a high number of MD trajectories in different complexes.

**Table 3.** Shows the total binding free energy and related term of all the six complexes subjected to MMGBSA analysis. All the energies are given in kcal/mol.

Complex name	MMGBSA				
	$\Delta$ vdW	$\Delta$ elec	$\Delta$ ps	$\Delta$ SASA	$\Delta$ G total
3CLpro-Saquinavir	-80.2350	0.0000	13.7916	-7.9627	-74.4061
3CLpro-5280805	-10.595	-26.061	54.8144	-3.6955	-29.486
3CLpro-5280445	-19.675	-22.019	33.119	-2.786	-16.342
3CLpro-5280343	-41.536	-11.714	25.747	-2.276	-17.184
3CLpro-5280863	-46.628	-1.1902	12.8929	-2.928	-10.315
3CLpro-5458190	-40.830	-8.972	22.1744	-1.508	-15.695

**Elec** = electrostatic energy;

**Ps** = polar solvation energy;

**SASA** = solvent-accessible surface area energy;

**vdW** = van der Waals energy;

**G Total** = total binding free energy;

**MMGBSA** = molecular mechanics generalized Born solvent accessibility.

the RMSD for the first 15 ns while remained uniformed for the rest of the simulation time. Thus, these results revealed the stable internal motions and negligible fluctuations during the course of the simulation. The differences in the RMSD of each system is due to the binding and unbinding of the ligand at different time intervals. Also, the systems with more stable behaviour show that the ligand remained intact, and the system entered the production phase soon when compared to the others. Aside, the binding of small molecules affects the system differently as the ligand-binding orientation changes over the simulation time.

### RMSF analysis

The RMSF depicts the flexibility at residues level. As shown in Figure 5, the pattern of flexibility is almost similar and was recorded around 1–4Å in all secondary components except loop regions with slightly fluctuated residues. However, active site residues seem stable in the course of the simulation, which is due to the ligand recognition by the ligand-binding regions. It can be seen that 3CLpro-Saquinavir and 3CLpro-5458190 showed an average RMSF of 2.5 Å with significant fluctuations in the regions 40–45, 90–110, 150–165, and 245–260. A similar pattern of fluctuation was also observed for systems including 3CLpro-5280805, 3CLpro-

5280445, and 3CLpro-5280863. However, the average RMSF remained below the 2 Å. Only the system 3CLpro-5280343 wed higher fluctuation than the rest, but the residual flexibility pattern was similar. The average RMSF for all the five systems was around 1–4Å, as clearly seen in Figure 5 (Left Panel). These findings here show that the target protein is stabilized by binding of all five chosen drugs docked against it. Thus the binding of ligand has significantly affected the residue fluctuation, which is due to the internal residues disturbed by the binding of different ligands, and this both correlated and non-correlated motions are affected. The secondary structure components are also given in Figure 5 (Right Panel).

### Radius of gyration

The radius of Gyration (RoG) conveys the information of stable and unstable folding protein while interacting with ligands. Less compactness (more unfolded) shows higher RoG values, whereas low RoG values indicate strong compactness and higher structural stiffness (more folded). Thus, RoG was determined to assess the system's compactness over time. As shown in Figure 6, the simulated complexes show gyration scores between 21 and 24Å. In the case of 3CLpro-Saquinavir, the gyration score for the initial (2000) frames was reported to be 22.50 Å. However, a little fluctuation between (2000–3000) frames was observed, but soon after 3500, the values become lower and uniform. In the case of 3CLpro-5280805, 3CLpro-5280445, 3CLpro-5280863, and 3CLpro-5458190 showed an average gyration of 22–22.50 Å. Similarly, 3CLpro-5280445 also showed similar fluctuation, but in the last few frames, the values fluctuated a little higher, which is assumed to be in an acceptable range. The binding and unbinding of ligands greatly affected the overall compactness of the complexes.

### Hydrogen bond occupancy

As given in Figure 7, in 3CLpro-Saquinavir, 3CLpro-5280805, and 3CLpro-5280343 complexes, the hydrogen bond with

His41 was reported in 87%, 65% and 39% of the trajectories. Hydrogen bond with Cys145 residue was reported in 65% trajectories only in the 3CLpro-Squanavir complex. Furthermore, Leu141 and Glu166 were found in almost all complexes. However, another important residue Gln189 was found in 76% of the 3CLpro-Squanavir trajectories, 36% in 3CLpro-5280805, while 21% in 3CLpro-TCM5280445 trajectories. Other active site residues were not detected in a significant population of the MD trajectories.

### Binding free energy

MM/GBSA, a popular approach, was used to estimate the binding free energy of all the six systems. The binding free energy determines the binding affinity between ligands and 3CLpro. Each energy term, including van der Waals energy, electrostatic energy, polar solvation energy, solvent accessible surface area energy, and total binding free energy of all the systems are given in Table 3. It can be seen that the 3CLpro-Saquinavir system possesses the highest total binding energy of  $-74.4061$  kcal/mol. Thus it confirms that Saquinavir, an anti-HIV drug that has been reported to inhibit HIV protease experimentally, possesses strong inhibitory effects against the 3CLpro of SARS-COV-2. Recently published results also shortlisted Saquinavir as a potential candidate, but they only performed 20 ns simulation (Khan et al., 2020), which could not reflect better results than what we revealed by adding 5-folds more simulation time.

Furthermore, the top five hits from TCM virtual screening results were also subjected to the free binding energy as reported by the virtual screening results TCM5280805 was reported with the best docking score and interaction. Herein, TCM5280805 also possesses the best total binding energy,  $29.486$  kcal/mol, against the 3CLpro. Also, the other hits from including TCM5280445, TCM5280343, TCM5280863, and TCM5458190 possess total binding energy of  $-16.342$  kcal/mol,  $-17.184$  kcal/mol,  $-10.315$  kcal/mol and  $-15.695$  kcal/mol. While the other energy terms such as van der Waals energy, electrostatic energy, polar solvation energy, solvent-accessible surface area are given in Table 3, thus these results strongly suggest that Saquinavir and TCM5280805 should be tested experimentally against the SARS-COV-2 at earliest.

### Discussion

To date, a total of 4,434,653 confirmed cases and 302,169 deaths are reported from the SARS-COV-2 epidemic, which indicates that the current viral treatment is not satisfactory, and more diverse studies are needed for the incorporation of various natural and FDA approved compounds for the effective treatment of SARS-COV-2. Further, our existing capacity for treating zoonotic coronavirus infections is still in the trial, and the available resources seem very limited to fight this life-threatening hazard. Although extensive research efforts have been initiated during 2003 and 2012 outbreaks of SARS and MERS-CoV, respectively, however, no effective drugs so far have been synthesized, nor the matter may be taken

seriously to prevent the future pandemics of zoonotic coronavirus. Drug repositioning is a 'universal strategy' for neglected diseases due to reduced number of clinical trial steps required could reduce the time and cost of the medicine to reach the market, existing pharmaceutical supply chains could facilitate the 'formulation and distribution' of the drug, the known possibility of combining with other drugs could enable more efficient treatment, Repositioning could encourage the development of 'new modes of action for old drugs and new types of medicines, eliminating 'activation obstacles' from early stages of study could allow the project to progress rapidly towards disease-oriented development (Pushpakom et al., 2019). One of the primary reasons why no prototype coronavirus inhibitor has progressed to the (early) preclinical stage so far is due to the transient nature of this epidemic. Like the SARS virus 17 years ago, the new SARS-CoV-2, and the new evolving coronaviruses that may continue to pose a threat to global public health in the future. Hence, discovering broad-spectrum inhibitors that can reduce the symptoms of human coronavirus infection remains a formidable subject of study. Considering the time-consuming process of designing and documenting antiviral medications, proven therapies for certain diseases may be the only fastest therapeutic choice for emerging infectious diseases. The prescription has ample experience and dosage for most of those medications that have been formulated, and their health and ADME properties are well known.

In this study, based on the results of bioinformatics analysis, we targeted 3CLpro from SARS-COV-2 using drugs repurposing (anti-HIV drugs) virtual drugs screening (TCM) approaches to shortlist the most potent compounds for the possible treatment. The results of the entire article stressed the potential inhibitory role of Saquinavir and TCM5280805, which are based on computer-based virtual drug screening. We have not conducted further in vivo and in vitro antiviral experiments yet, because we want to share our results with scientists in anti-SARS-CoV-2 research as soon as possible. This study will help to repurpose drug design, perform in vivo and in vitro evaluations for candidate drugs obtained in this study, and prepare for clinical trial applications.

### Conclusion

3C-like protease (3CLpro), also called the main protease, is an attractive target for the treatment of SARS-COV-2 because of its role in the viral replication cycle. The current study focused on structure based approaches repurposed anti-HIV drugs and Screened Traditional Chinese Medicines databases against the active site residues of 3CLPro. Initial analysis such as molecular docking scores and interactions with important residues shortlisted one drug (Saquinavir) from anti-HIV drugs while five compounds from TCM database. These compounds were then subjected to molecular dynamics simulation and post-simulation analysis. Among the six complexes subjected to molecular dynamics simulation Saquinavir, TCM5280805 showed the highest hydrogen bond occupancy. The rest were also found to have good activity against the

3CLPro. In addition, the bioactivity of these compounds were predicted which reported Saquinavir as strong potential inhibitor followed by the others. Binding Free energy calculations of all the complexes suggested that these compounds significantly interacting and binds with the receptor. Thus, here from all the analyses, we suggest that Saquinavir and TCM5280805 should be tested experimentally for possible treatment of SARS-CoV-2.

### Authors contribution

AK, ZB, MK, and SSA conceptualized the study and did the analysis. AA, MS, SS wrote the manuscript. AK, SS and SSA revised the manuscript and improved the write-up. DQW is an academic supervisor. He supervised the study.

### Disclosure statement

The authors declare no conflict of interest.

### Funding

Dong-Qing Wei is supported by the grants from the Key Research Area Grant 2016YFA0501703 of the Ministry of Science and Technology of China, the National Natural Science Foundation of China (Contract no. 61832019, 61503244), the Natural Science Foundation of Henan Province (162300410060) and Joint Research Funds for Medical and Engineering and Scientific Research at Shanghai Jiao Tong University (YG2017ZD14). The computations were partially performed at the Center for High-Performance Computing, Shanghai Jiao Tong University.

### ORCID

Muhammad Tahir Khan  <http://orcid.org/0000-0003-1158-2133>  
Mazhar Khan  <http://orcid.org/0000-0003-1158-2133>

### References

Bosch, B. J., van der Zee, R., de Haan, C. A., & Rottier, P. J. (2003). The coronavirus spike protein is a class I virus fusion protein: Structural and functional characterization of the fusion core complex. *Journal of Virology*, 77(16), 8801–8811. <https://doi.org/10.1128/jvi.77.16.8801-8811.2003>

Case, D. A., Cheatham, T. E., Darden, T., Gohlke, H., Luo, R., Merz, K. M., Onufriev, A., Simmerling, C., Wang, B., & Woods, R. J. (2005). The Amber biomolecular simulation programs. *Journal of Computational Chemistry*, 26(16), 1668–1688. <https://doi.org/10.1002/jcc.20290>

Chan, J. F. W., Chan, K.-H., Kao, R. Y. T., To, K. K. W., Zheng, B.-J., Li, C. P. Y., Li, P. T. W., Dai, J., Mok, F. K. Y., Chen, H., Hayden, F. G., & Yuen, K.-Y. (2013). Broad-spectrum antivirals for the emerging Middle East respiratory syndrome coronavirus. *The Journal of Infection*, 67(6), 606–616. <https://doi.org/10.1016/j.jinf.2013.09.029>

Chen, F., Liu, H., Sun, H., Pan, P., Li, Y., Li, D., & Hou, T. (2016). Assessing the performance of the MM/PBSA and MM/GBSA methods. 6. Capability to predict protein-protein binding free energies and re-rank binding poses generated by protein-protein docking. *Physical Chemistry Chemical Physics: PCCP*, 18(32), 22129–22139. <https://doi.org/10.1039/c6cp03670h>

Chen, H., & Du, Q. (2020). Potential natural compounds for preventing SARS-CoV-2 (2019-nCoV) infection. *Preprints*, 92, 1–17.

Chen, Y., Liu, Q., & Guo, D. (2020). Emerging coronaviruses: Genome structure, replication, and pathogenesis. *Journal of Medical Virology*, 92(4), 418–423. <https://doi.org/10.1002/jmv.25681>

Cheng, V. C., Lau, S. K., Woo, P. C., & Yuen, K. Y. (2007). Severe acute respiratory syndrome coronavirus as an agent of emerging and re-emerging infection. *Clinical Microbiology Reviews*, 20(4), 660–694. <https://doi.org/10.1128/CMR.00023-07>

Dai, W., Zhang, B., Jiang, X.-M., Su, H., Li, J., Zhao, Y., Xie, X., Jin, Z., Peng, J., Liu, F., Li, C., Li, Y., Bai, F., Wang, H., Chen, X., Cen, X., Hu, S., Yang, X., Wang, J., ... Liu, H. (2020). Structure-based design, synthesis and biological evaluation of peptidomimetic aldehydes as a novel series of antiviral drug candidates targeting the SARS-CoV-2 main protease. *bioRxiv*, 1–17.

de Groot, R. J., Baker, S. C., Baric, R. S., Brown, C. S., Drosten, C., Enjuanes, L., Fouchier, R. A. M., Galiano, M., Gorbalenya, A. E., Memish, Z. A., Perlman, S., Poon, L. L. M., Snijder, E. J., Stephens, G. M., Woo, P. C. Y., Zaki, A. M., Zambon, M., & Ziebuhr, J. (2013). Commentary: Middle East respiratory syndrome coronavirus (MERS-CoV): Announcement of the Coronavirus Study Group. *Journal of Virology*, 87(14), 7790–7792. <https://doi.org/10.1128/JVI.01244-13>

de Wilde, A. H., Jochmans, D., Posthuma, C. C., Zevenhoven-Dobbe, J. C., van Nieuwkoop, S., Bestebroer, T. M., van den Hoogen, B. G., Neyts, J., & Snijder, E. J. (2014). Screening of an FDA-approved compound library identifies four small-molecule inhibitors of Middle East respiratory syndrome coronavirus replication in cell culture. *Antimicrobial Agents and Chemotherapy*, 58(8), 4875–4884. <https://doi.org/10.1128/AAC.03011-14>

Dyall, J., Coleman, C. M., Hart, B. J., Venkataraman, T., Holbrook, M. R., Kindrachuk, J., Johnson, R. F., Olinger, G. G., Jahrling, P. B., Laidlaw, M., Johansen, L. M., Lear-Rooney, C. M., Glass, P. J., Hensley, L. E., & Frieman, M. B. (2014). Repurposing of clinically developed drugs for treatment of Middle East respiratory syndrome coronavirus infection. *Antimicrobial Agents and Chemotherapy*, 58(8), 4885–4893. <https://doi.org/10.1128/AAC.03036-14>

Hernandez, J. J., Prysizlak, M., Smith, L., Yanchus, C., Kurji, N., Shahani, V. M., & Molinski, S. V. (2017). Giving drugs a second chance: Overcoming regulatory and financial hurdles in repurposing approved drugs as cancer therapeutics. *Frontiers in Oncology*, 7, 273. <https://doi.org/10.3389/fonc.2017.00273>

Hou, T., Li, N., Li, Y., & Wang, W. (2012). Characterization of domain-peptide interaction interface: prediction of SH3 domain-mediated protein-protein interaction network in yeast by generic structure-based models. *Journal of Proteome Research*, 11(5), 2982–2995. <https://doi.org/10.1021/pr3000688>

Huang, C., Wang, Y., Li, X., Ren, L., Zhao, J., Hu, Y., Zhang, L., Fan, G., Xu, J., Gu, X., Cheng, Z., Yu, T., Xia, J., Wei, Y., Wu, W., Xie, X., Yin, W., Li, H., Liu, M., ... Cao, B. (2020). Clinical features of patients infected with 2019 novel coronavirus in Wuhan. *The Lancet*, 395(10223), 497–506. [https://doi.org/10.1016/S0140-6736\(20\)30183-5](https://doi.org/10.1016/S0140-6736(20)30183-5)

Jin, Z., Du, X., Xu, Y., Deng, Y., Liu, M., Zhao, Y., Zhang, B., Li, X., Zhang, L., Peng, C., Duan, Y., Yu, J., Wang, L., Yang, K., Liu, F., Jiang, R., Yang, X., You, T., Liu, X., ... Yang, H. (2020). Structure of Mpro from COVID-19 virus and discovery of its inhibitors. *bioRxiv*, 1–33.

Khan, A., Kaushik, A. C., Ali, S. S., Ahmad, N., & Wei, D.-Q. (2019). Deep-learning-based target screening and similarity search for the predicted inhibitors of the pathways in Parkinson's disease. *RSC Advances*, 9(18), 10326–10339. <https://doi.org/10.1039/C9RA01007F>

Khan, A., Saleem, S., Idrees, M., Ali, S. S., Junaid, M., Kaushik, A. C., & Wei, D.-Q. (2018). Allosteric ligands for the pharmacologically important Flavivirus target (NS5) from ZINC database based on pharmacophoric points, free energy calculations and dynamics correlation. *Journal of Molecular Graphics & Modelling*, 82, 37–47. <https://doi.org/10.1016/j.jmgm.2018.03.004>

Khan, S. A., Zia, K., Ashraf, S., Uddin, R., & Ul-Haq, Z. (2020). Identification of Chymotrypsin-like protease inhibitors of SARS-CoV-2 via integrated computational approach. *Journal of Biomolecular Structure and Dynamics*, 38, 1–13.

Kim, A. E., Dintaman, J. M., Waddell, D. S., & Silverman, J. A. (1998). Saquinavir, an HIV protease inhibitor, is transported by P-glycoprotein. *The Journal of Pharmacology and Experimental Therapeutics*, 286(3), 1439–1445.

Lau, S. K. P., Woo, P. C. Y., Li, K. S. M., Huang, Y., Tsoi, H.-W., Wong, B. H. L., Wong, S. S. Y., Leung, S.-Y., Chan, K.-H., & Yuen, K.-Y. (2005).

- Severe acute respiratory syndrome coronavirus-like virus in Chinese horseshoe bats. *Proceedings of the National Academy of Sciences of the United States of America*, 102(39), 14040–14045. <https://doi.org/10.1073/pnas.0506735102>
- Lee, N., Hui, D., Wu, A., Chan, P., Cameron, P., Joynt, G. M., Ahuja, A., Yung, M. Y., Leung, C. B., To, K. F., Lui, S. F., Szeto, C. C., Chung, S., & Sung, J. J. Y. (2003). A major outbreak of severe acute respiratory syndrome in Hong Kong. *The New England Journal of Medicine*, 348(20), 1986–1994. <https://doi.org/10.1056/NEJMoa030685>
- Lerner, M., & Carlson, H. (2006). *APBS plugin for PyMOL*. University of Michigan.
- Miller III, B. R., McGee, T. D., Jr, Swails, J. M., Homeyer, N., Gohlke, H., & Roitberg, A. E. (2012). MMPBSA.py: An efficient program for end-state free energy calculations. *Journal of Chemical Theory and Computation*, 8(9), 3314–3321. <https://doi.org/10.1021/ct300418h>
- Omran, A. S., Saad, M. M., Baig, K., Bahloul, A., Abdul-Matin, M., Alaidaroos, A. Y., Almakhlafi, G. A., Albarrak, M. M., Memish, Z. A., & Albarrak, A. M. (2014). Ribavirin and interferon alfa-2a for severe Middle East respiratory syndrome coronavirus infection: A retrospective cohort study. *The Lancet. Infectious Diseases*, 14(11), 1090–1095. [https://doi.org/10.1016/S1473-3099\(14\)70920-X](https://doi.org/10.1016/S1473-3099(14)70920-X)
- Price, D. J., & Brooks III, C. L. (2004). A modified TIP3P water potential for simulation with Ewald summation. *The Journal of Chemical Physics*, 121(20), 10096–10103. <https://doi.org/10.1063/1.1808117>
- Pushpakom, S., Iorio, F., Eyers, P. A., Escott, K. J., Hopper, S., Wells, A., Doig, A., Guilliams, T., Latimer, J., McNamee, C., Norris, A., Sanseau, P., Cavalla, D., & Pirmohamed, M. (2019). Drug repurposing: Progress, challenges and recommendations. *Nature Reviews. Drug Discovery*, 18(1), 41–58. <https://doi.org/10.1038/nrd.2018.168>
- Release, S. (2017). *Maestro*. Schrödinger, LLC.
- Reusken, C. B., Haagmans, B. L., Müller, M. A., Gutierrez, C., Godeke, G.-J., Meyer, B., Muth, D., Raj, V. S., Vries, L. S.-D., Corman, V. M., Drexler, J.-F., Smits, S. L., El Tahir, Y. E., De Sousa, R., van Beek, J., Nowotny, N., van Maanen, K., Hidalgo-Hermoso, E., Bosch, B.-J., ... Koopmans, M. P. (2013). Middle East respiratory syndrome coronavirus neutralising serum antibodies in dromedary camels: A comparative serological study. *The Lancet Infectious Diseases*, 13(10), 859–866. [https://doi.org/10.1016/S1473-3099\(13\)70164-6](https://doi.org/10.1016/S1473-3099(13)70164-6)
- Roe, D. R., & Cheatham III, T. E. (2013). PTRAJ and CPPTRAJ: Software for processing and analysis of molecular dynamics trajectory data. *Journal of Chemical Theory and Computation*, 9(7), 3084–3095. <https://doi.org/10.1021/ct400341p>
- Rose, P. W., Prlić, A., Altunkaya, A., Bi, C., Bradley, A. R., Christie, C. H., Di Costanzo, L., Duarte, J., Dutta, S., Feng, Z., Green, R. K., Goodsell, D. S., Hudson, B., Karlo, T., Lowe, R., Peisach, E., Randle, C., Rose, A. S., Shao, C., ... Burley, S. K. (2016). The RCSB protein data bank: Integrative view of protein, gene and 3D structural information. *Nucleic Acids Research*, 45(D1), D271–D281.
- Rothan, H. A., & Byrareddy, S. N. (2020). The epidemiology and pathogenesis of coronavirus disease (COVID-19) outbreak. *Journal of Autoimmunity*, 109, 102433. <https://doi.org/10.1016/j.jaut.2020.102433>
- Schrodinger, L. (2011). *Schrodinger software suite* (p. 670). Schrödinger, LLC.
- Sleigh, S. H., & Barton, C. L. (2010). Repurposing strategies for therapeutics. *Pharmaceutical Medicine*, 24(3), 151–159. <https://doi.org/10.1007/BF03256811>
- Sun, H., Li, Y., Tian, S., Xu, L., & Hou, T. (2014). Assessing the performance of MM/PBSA and MM/GBSA methods. 4. Accuracies of MM/PBSA and MM/GBSA methodologies evaluated by various simulation protocols using PDBbind data set. *Physical Chemistry Chemical Physics: PCCP*, 16(31), 16719–16729. <https://doi.org/10.1039/c4cp01388c>
- Ul Qamar, M. T., Alqahtani, S. M., Alamri, M. A., & Chen, L.-L. (2020). Structural basis of SARS-CoV-2 3CLpro and anti-COVID-19 drug discovery from medicinal plants. *Journal of Pharmaceutical Analysis*, 10, 1–7.
- Wang, Y., Khan, A., Chandra Kaushik, A., Junaid, M., Zhang, X., & Wei, D.-Q. (2019). The systematic modeling studies and free energy calculations of the phenazine compounds as anti-tuberculosis agents. *Journal of Biomolecular Structure & Dynamics*, 37(15), 4051–4069. <https://doi.org/10.1080/07391102.2018.1537896>
- Wishart, D. S., Feunang, Y. D., Guo, A. C., Lo, E. J., Marcu, A., Grant, J. R., Sajed, T., Johnson, D., Li, C., Sayeeda, Z., Assempour, N., Iynkkaran, I., Liu, Y., Maciejewski, A., Gale, N., Wilson, A., Chin, L., Cummings, R., Le, D., ... Wilson, M. (2018). DrugBank 5.0: a major update to the DrugBank database for 2018. *Nucleic Acids Research*, 46(D1), D1074–D1082. <https://doi.org/10.1093/nar/gkx1037>
- Yang, Y., Islam, M. S., Wang, J., Li, Y., & Chen, X. (2020). Traditional Chinese medicine in the treatment of patients infected with 2019-new coronavirus (SARS-CoV-2): a review and perspective. *International Journal of Biological Sciences*, 16(10), 1708–1717. <https://doi.org/10.7150/ijbs.45538>
- Zaki, A. M., Van Boheemen, S., Bestebroer, T. M., Osterhaus, A. D., & Fouchier, R. A. (2012). Isolation of a novel coronavirus from a man with pneumonia in Saudi Arabia. *The New England Journal of Medicine*, 367(19), 1814–1820. <https://doi.org/10.1056/NEJMoa1211721>
- Zhu, N., Zhang, D., Wang, W., Li, X., Yang, B., Song, J., Zhao, X., Huang, B., Shi, W., Lu, R., Niu, P., Zhan, F., Ma, X., Wang, D., Xu, W., Wu, G., Gao, G. F., & Tan, W. (2020). A novel coronavirus from patients with pneumonia in China, 2019. *The New England Journal of Medicine*, 382(8), 727–733.
- Zumla, A., Chan, J. F., Azhar, E. I., Hui, D. S., & Yuen, K.-Y. (2016). Coronaviruses - drug discovery and therapeutic options. *Nature Reviews. Drug Discovery*, 15(5), 327–347. <https://doi.org/10.1038/nrd.2015.37>